1521-0103/383/1/56–69$35.00
THE JOURNAL OF PHARMACOLOGY AND EXPERIMENTAL THERAPEUTICS

dx.doi.org/10.1124/jpet.121.001026
J Pharmacol Exp Ther 383:56–69, October 2022

Modulation of Ligand-Gated Glycine Receptors Via Functional Monoclonal Antibodies[S]

Jeffrey R. Simard, Klaus Michelsen, Yan Wang, Chunhua Yang, Beth Youngblood, Barbara Grubinska, Kristin Taborn, Daniel J. Gillie, Kevin Cook, Kyu Chung, Alexander M. Long, Brian E. Hall, Paul L. Shaffer, Robert S. Foti, and Jacinthe Gingras

Departments of Neuroscience (J.R.S., C.Y., B.Y. B.G., K.T., D.J.G., J.G.), Molecular Engineering (K.M., A.M.L., P.L.S.), Protein Technologies (Y.W., B.E.H.), and Pharmacokinetics and Drug Metabolism (R.S.F.), Amgen Research, Cambridge, Massachusetts; and Department of Pharmacokinetics and Drug Metabolism, Amgen Research, 1120 Veterans Boulevard, South San Francisco, California (K.Co., K.Ch.)

Received November 17, 2021; accepted July 19, 2022

ABSTRACT

Ion channels are targets of considerable therapeutic interest to address a wide variety of neurologic indications, including pain perception. Current pharmacological strategies have focused mostly on small molecule approaches that can be limited by selectivity requirements within members of a channel family or superfamily. Therapeutic antibodies have been proposed, designed, and characterized to alleviate this selectivity limitation; however, there are no Food and Drug Administration-approved therapeutic antibody-based drugs targeting ion channels on the market to date. Here, in an effort to identify novel classes of engineered ion channel modulators for potential neurologic therapeutic applications, we report the generation and characterization of six (EC_{50} < 25nM) Cys-loop receptor family monoclonal antibodies with modulatory function against rat and human glycine receptor alpha 1 (GlyRα1) and/or GlyRα3. These antibodies have activating (i.e., positive modulator) or inhibiting (i.e., negative modulator) profiles. Moreover, GlyRα3 selectivity was successfully achieved for two of the three positive modulators identified. When dosed intravenously, the antibodies achieved sufficient brain exposure to cover their calculated in vitro EC_{50} values. When compared head-to-head at identical exposures, the GlyRα3-selective antibody showed a more desirable safety profile over the nonselective antibody, thus demonstrating, for the first time, an advantage for GlyRα3-selectivity. Our data show that ligand-gated ion channels of the glycine receptor family within the central nervous system can be functionally modulated by engineered biologics in a dose-dependent manner and that, despite high protein homology between the alpha subunits, selectivity can be achieved within this receptor family, resulting in future therapeutic candidates with more desirable drug safety profiles.

SIGNIFICANCE STATEMENT

This study presents immunization and multiplatform screening approaches to generate a diverse library of functional antibodies (agonist, potentiator, or inhibitory) raised against human glycine receptors (GlyRs). This study also demonstrates the feasibility of acquiring alpha subunit selectivity, a desirable therapeutic profile. When tested in vivo, these tool molecules demonstrated an increased safety profile in favor of GlyRα3-selectivity. These are the first reported functional GlyR antibodies that may open new avenues to treating central nervous system diseases with subunit selective biologics.

Introduction

Ion channels play a critical role in membrane excitability, secretion, cell migration, and gene transcription. Indeed, more than 400 ion channel genes have been identified to date (Overington et al., 2006; Bagal and Bungay, 2012), making them an important target-class for drug discovery. Many have been validated as potential therapeutic targets covering a vast array of neuronal diseases. Small molecule approaches have been favored for centrally located targets due to the requirement of crossing the blood brain barrier (BBB), but peripherally restricted ion channels have been interrogated with biologics such as functional (inhibiting) antibodies or biologic toxins (Beck et al., 2010; Bosmans and Swartz, 2010). To date, no approved therapeutic antibody-based molecule has been developed for ion channels, reiterating the difficulties of such an approach and the associated limitations with methods of delivery. In particular, we focus on the near absence of

This work received no external funding. All authors were employees of Amgen, Inc., which was the sole sponsor of the research.
No author has an actual or perceived conflict of interest with the contents of this article.
dx.doi.org/10.1124/jpet.121.001026.
[S] This article has supplemental material available at jpet.aspetjournals.org.

ABBREVIATIONS: BBB, blood brain barrier; CNS, central nervous system; DDM, n-dodecyl β-D-maltoside; FAb, fragmented monoclonal antibody; FACS, fluorescence-activated cell sorting; FESC, fluorescent-detection size-exclusion chromatography; FLIPR, fluorescence imaging plate reader; GlyR, glycine receptor; GlyRα1, homopentameric glycine receptor alpha 1; GlyRα3, homopentameric glycine receptor alpha 3; GlyRα1β, heteropentameric glycine receptor alpha 1 with beta subunits; GlyRα3β, heteropentameric glycine receptor alpha 3 with beta subunits; HTS, high-throughput screening; mAb, full-length monoclonal antibody; MP, membrane potential; OPA, open-field assay; POC, percent of control; SPR, surface plasmon resonance.

functional therapeutic antibodies for glycine receptors (GlyRs).

Glycine receptors (GlyRs) are chloride-conducting ion channels belonging to the Cys-loop superfamily and are comprised of five subunits arranged into pentamers around a central ion pore with ligand binding sites located at subunit domain interfaces (Hibbs and Gouaux, 2011; Huang et al., 2015). Each subunit consists of a large extracellular binding domain and four transmembrane helices with the transmembrane 2 helix lining the central pore cavity. The alpha (α) subunits are required for functional chloride conductivity (Betz and Laube, 2006). All α isoforms can arrange into homomeric pentamers or combine with beta (β) subunits to form heteromeric Gly$\alpha\beta$ channels. Although expression of the β subunit alone does not lead to a functional channel, the β subunit has been shown to modulate agonist affinities and interact strongly with the intracellular protein gephyrin to facilitate postsynaptic clustering of GlyR heteropentamers (for review see Tyagarajan and Fritschy, 2014; Burgos et al., 2016). The protein sequences of the full-length human GlyRα1 and α3 subunits are ~93% similar, with the sequence identity increasing to ~97% within the extracellular binding domain, making selective targeting of these receptors challenging. For this reason, selective tools necessary to characterize these various channel subtypes and better resolve their precise pharmacology have been lacking.

In the central nervous system (CNS), glycine is one of two major inhibitory neurotransmitters modulating transduction of both sensory and motor signals. Glycinergic interneurons synapse onto second order spinal neurons that receive direct input from peripheral sensory neurons (of which cell bodies are located in the dorsal root ganglia) and have been demonstrated to be key players in the modulation of pain and itch processing (Foster et al., 2015). Their enriched distribution in the spinal cord and brainstem makes them an attractive therapeutic target class for modulation of neuronal circuitry (Harvey et al., 2004). Indeed, GlyRα3 has been reported to be implicated in the processing of inflammatory pain (Ahmadi et al., 2002; Harvey et al., 2004; Lynch and Callister, 2006; Werynska et al., 2021), and its potential therapeutic role in a wider variety of pain perception (including chronic pain) has been demonstrated by the analgesic effects of cannabis and its primary psychoactive component Δ9–tetrahydrocannabinol (Hejazi et al., 2006; Xiong et al., 2011), as well as positive allosteric modulation of GlyRs in a model of neuropathic pain (Bregman et al., 2017; Huang et al., 2017) (also see reviews: Zeilhofer et al., 2018; Zeilhofer et al., 2021). Additional reported positive modulators of GlyRs include divalent cations (e.g., Zn^{2+}), glutamatergic ligands, neuroactive steroids, general anesthetics, n-alcohols and propofol derivatives, plant alkaloids such as tropeines and gelsimine, and ginkolic acid (Yévenes and Zeilhofer, 2011; Maleeva et al., 2015a, 2015b; Shalaly et al., 2015). Conversely, the GlyR antagonist strychnine heightens painful response by blocking stimulation of the inhibitory pain control pathway by glycine (Beyer et al., 1985; Yaksh, 1989; Loomis et al., 2001).

Here, we report the generation and characterization of six rat/human GlyRs mouse monoclonal antibodies with positive and negative receptor modulation profiles. The ability of these antibodies to modulate GlyRα3/1(β) subtypes or to selectively modulate GlyRα3 activity was demonstrated via an in vitro cell-based membrane potential (MP) dye high-throughput screening (HTS) assay using corresponding human (HEK293T) stable cell lines. In addition, we demonstrate that selectivity favoring GlyRα3 over GlyRα1 offers a more desirable safety profile when dosed head-to-head in vivo (in rats) at the same dose and exposure. These new tools, combined with our current understanding of chronic pain-related CNS target engagement for GlyRs, support the investigation of selective monoclonal antibody approaches to target these receptors.

Materials and Methods

Generation of Stable Human GlyR Cell Lines. HEK293T cells stably expressing full-length human GlyRα3β, GlyRα1β, GlyRα1, or GlyRα3 were used in these studies and have been described previously (Huang et al., 2015, 2017). Briefly, the α3, α1, and β subunits of the human glycine receptor were individually subcloned into the pcDNA3.1 vectors containing various antibiotic selection cassettes (Thermo Fisher Scientific, Waltham, MA) and stably transfected into HEK293T cells grown in cell culture medium (Dulbecco's modified Eagle's medium supplemented with 10% v/v heat-inactivated FBS, 100 units Penicillin, 100 units streptomycin, 29.2 mg/ml of L-glutamine). During the clonal selection, picrotoxin was used to characterize the GlyR homopentameric and heteromeric cell lines and confirmed the absence of significant native GlyR β subunit proteins, which have been reportedly expressed in HEK293 cells (Thomas and Smart, 2005). Despite being expressed in the same HEK293T cellular background, we observed a ~1000X weaker picrotoxin inhibition potency in cells expressing heteropentameric GlyRα3β compared with cells expressing homopentameric GlyRα3. Although we cannot rule out the presence of trace levels of endogenous GlyR β subunit proteins, the picrotoxin results suggest that their influence on GlyR channel profiles is not significant.

For screening purposes, the cells were cultured and prepared as follows. After 48–72 hours of incubation at 37°C, 5% v/v CO_2 and 95% humidity, cells were seeded using single cell dilution into 96 well plates containing cell culture media with the corresponding antibiotic selection; cells transfected with subunit α3 and α1 DNA were selected using hygromycin, and the β subunit expressing cells were selected using 100 μg/ml zeocin (Thermo Fisher Scientific, Waltham, MA). The stable clones were expanded in fresh medium containing selective antibiotic. Protein expression was confirmed by western blot and functional assay testing.

Human GlyRα3 and GlyRα1 Protein Constructs, Expression, and Purification. Expression and purification of homopentameric human GlyRα3 and GlyRα1 protein was carried out as described previously (Huang et al., 2015, 2017) using the Bac-to-Bac system (Life Technologies). Briefly, the recombinant baculoviruses containing mammalian GlyRα3 or GlyRα1 sequences were generated, and expression was carried out in baculovirus transduced Sf9 insect cells grown in SFX-Insect Cell Culture Medium (Hyclone) at 27°C for 72 hours. Cells were harvested by centrifugation and disrupted in a microfluidizer, and the homogenate was clarified by centrifugation at 10,000 g. Crude membranes were then collected by centrifugation at 125,000 g. The membranes were mechanically homogenized and solubilized in 0.2 g n-dodecyl β-D-maltoside (DDM) per gram of membranes in 20 mM Tris pH 8.0, 150 mM NaCl, 0.5% protease inhibitors cocktail and then centrifuged again at 125,000 g. The supernatant was bound to strep affinity resin (IBA GmbH), washed with 20 mM Tris pH 8.0, 150 mM NaCl, 1 mM DDM, and eluted with 20 mM Tris pH 8.0, 150 mM NaCl, 1 mM DDM, and 5 mM desthiobiotin. Eluted protein fractions were pooled together, concentrated, and further purified by gel filtration in 20 mM Tris pH 8.0, 150 mM NaCl, and 1 mM DDM. All purification steps were performed at 4°C.

Generation of Full-Length and Fragmented Monoclonal Antibodies. Mouse monoclonal antibodies were originally generated against human GlyRα3 protein for the intended purpose of stabilizing purified GlyR proteins for crystallization. Recombinantly expressed and purified human GlyRα3 in detergent micelles was used to immunize adult wild type mice, and initial hybridoma screening was done

TABLE 1
Correlation of FLIPR assay functional response for full-length (mAb) and fragmented (FAb) mouse monoclonal antibodies on various cell lines stably expressing human GlyR channelsEC_{50}/IC_{50} values were extrapolated from a sigmoidal Hill fit (four parameter) of a plot of at least three independent dose response experiments.

	Full-Length Abs Activity EC_{50} (nM)		FAbs Activity EC_{50} (nM)			
mAb	GlyR$\alpha3\beta$	GlyR$\alpha1\beta$	GlyR$\alpha3\beta$	GlyR$\alpha1\beta$	GlyR$\alpha3$	GlyR$\alpha1$
14E3	8.1	11.2	41.7	44.5	19.9	39.0
15B5	11.2	4.9	—	—	—	—
17A1	18.1	42.3	—	—	—	—
19C8	6.1	8.9	15.5	27.6	6.7	25.3
9A11	5.3	nd	14.3	nd	49.5	nd
17D2	11.9	nd	—	—	—	—
6C6	N/A	N/A	—	—	—	—
10E2	N/A	N/A	—	—	—	—

nd, not determined due to inactivity on indicated cell lines.

by native ELISA using Ni-NTA plates (Qiagen) and buffers containing detergent. To limit the number of antibodies recognizing linear epitopes, hybridomas that showed response against 8 M urea denatured protein were eliminated. Specificity of the antibody for properly folded GlyR$\alpha3$ was assayed by fluorescent-detection size-exclusion chromatography (FSEC), assessing in-solution binding to a GlyR$\alpha3$ - green fluorescent protein (GFP) fusion. GFP was incorporated in the loop between transmembrane helices 3 and 4. Finally, to further eliminate hybridomas that bind to linear epitopes, those that showed signal in SDS-PAGE western blots against GlyR$\alpha3$ were also eliminated. Hybridoma cell lines were dilution cloned to ensure monoclonality. A total of six monoclonal antibodies were generated, and each was purified from supernatants by mercaptoethylpyridine and protein A chromatography. Fragmented monoclonal antibody (FAb) fragments were generated by papain digestion and purified by ion exchange chromatography to remove Fc and undigested material.

To facilitate the investigation of these antibodies on GlyR channel function described here, molar concentrations were determined by first measuring the concentration of each stock solution using either a Bradford or bicinchoninic acid (BCA) assay and extrapolating stock concentration value from a bovine serum albumin standard curve followed by the UV absorbance at 280 nm (A_{280}) measurement of a serially diluted antibody or FAb to determine the molar extinction coefficient (ε). The molar extinction coefficient was calculated by plotting A_{280} versus concentration and taking the slope of a linear fit. Working solutions of each antibody or FAb were made fresh prior to each experiment, and concentrations were determined using Beer's Law and the respective experimentally determined molar extinction coefficient values. A full list of fragmented and full-length mouse monoclonal antibodies against human GlyR can be found in Table 1.

Functional Testing in Fluorescence Imaging Plate Reader Assay. We applied a high-throughput fluorescence imaging plate reader (FLIPR) MP Dye Assay (Jensen and Kristiansen, 2004) to assess the ability of GlyR antibodies and FAbs to modulate the net membrane potential of GlyR expressing HEK293T cells, as described previously (Huang et al., 2015, 2017). Briefly, HEK293T cells stably expressing full-length human GlyR$\alpha1\beta$, GlyR$\alpha3\beta$, GlyR$\alpha1$, or GlyR$\alpha3$ were cultured in cell culture medium (minimum Eagle's medium supplemented with 10% v/v qualified heat-inactivated FBS, 100 units penicillin, 100 units streptomycin, 29.2 mg/ml of L-glutamine) under standard cell culture conditions of 37°C, 5% v/v CO_2, and 95% humidity. Cells were grown in T 225 cm^2 culture flasks to a density of approximately 8×10^7 cells and harvested after approximately 4 days by briefly washing with Dulbecco's phosphate-buffer saline (DPBS) followed by addition of Cell Dissociation Buffer (enzyme-free PBS; Gibco, Waltham, MA) for 2 minutes. Alternatively, rat GlyR$\alpha1$ or GlyR$\alpha3$ were transiently expressed in HEK293T cells using BacMam system. Parental HEK293T cells were cultured and harvested as described above, followed by incubation with a titered baculovirus stock to enable transient overnight expression of each rat channel subtype. For all assays, the concentration of cells in suspension was adjusted to 4.80×10^5 cells/ml in cell plating medium (minimum Eagle's medium with 10% dialyzed FBS, 100 units Penicillin, 100 units streptomycin, 0.29 mg/ml of L-glutamine and 10 mM HEPES pH 7.4). Using a Multidrop Combi, 25 μl of cell suspension [stably (human) or transiently (rat) expressing GlyRs] was dispensed into Corning CellBIND 384-well ViewPlates. Cell culture plates were then incubated at 37°C overnight under the standard cell culture conditions described above. The next day (~18–24 hours after plating), 5 μl of 6X MP blue dye for monitoring changes in membrane potential was dispensed into each cell culture plate using a Thermo Multidrop Combi (prepared in assay buffer at 6X the manufacturer's recommended final concentration). The cell plates were then incubated at 37°C for 30 minutes and then allowed to equilibrate to room temperature for an additional 30 minutes.

All mouse monoclonal antibodies and FAb fragments were first tested in the absence of glycine in the FLIPR assay to determine whether they could activate the channel (i.e., agonist-like). Dose response plates containing a 1:2 stepwise dilution series of each antibody and FAb were prepared in low-chloride assay buffer (10 mM HEPES, 60 mM NaCl, 5 mM KCl, 2 mM $MgCl_2$, 1 mM $CaCl_2$, 10 mM D-glucose, 160 mM D-mannitol, and 2 M KOH solution to adjust pH to 7.4) supplemented with 2% v/v DMSO in standard 384-well polypropylene plates. Antibodies that did not activate GlyRs on their own were then tested with EC_{10} glycine (10 μM) added to the buffer to determine whether they could potentiate the EC_{10} glycine response. All full-length antibodies and FAbs were tested up to a final maximum concentration of 2 μM. The MP dye assay was carried out on FLIPR Tetra, which transferred 10 μl from the 4X dose response plate containing antibodies or FAbs (+/− EC_{10} glycine) and added it to the 30 μl volume in each well of the cell plate containing MP Blue Dye. Fluorescence emission (510–545 nm/565–625 nm excitation/emission filter set, excitation intensity = 40%, camera gain = 50, and an exposure time of 0.4 seconds) was measured in real-time to detect changes in membrane potential. The net cell membrane potential changes upon activation of GlyR channels and results in the increased efflux of Cl^- ions out of the cell down a concentration gradient and a robust increase in fluorescence signal. Fluorescence response was monitored out to 60 minutes to ensure that equilibrium was reached.

Antibodies that did not activate or potentiate GlyR channels within the first 60 minutes were subsequently exposed to EC_{70} glycine to determine whether these antibodies instead elicited the inhibition of glycine-induced channel activation. The high concentration of glycine was prepared at 5X in the Assay Buffer, and the FLIPR Tetra was used to transfer 10 μl of glycine to the plate containing cells pretreated for 60 minutes with each antibody or FAb. Owing to the rapid activation of GlyR channels by added glycine, real-time fluorescence changes were carried out for an additional 2 minutes to capture the full response. Where indicated, blockade of channel activation by antibodies was achieved by codosing the small molecule GlyR inhibitor strychnine

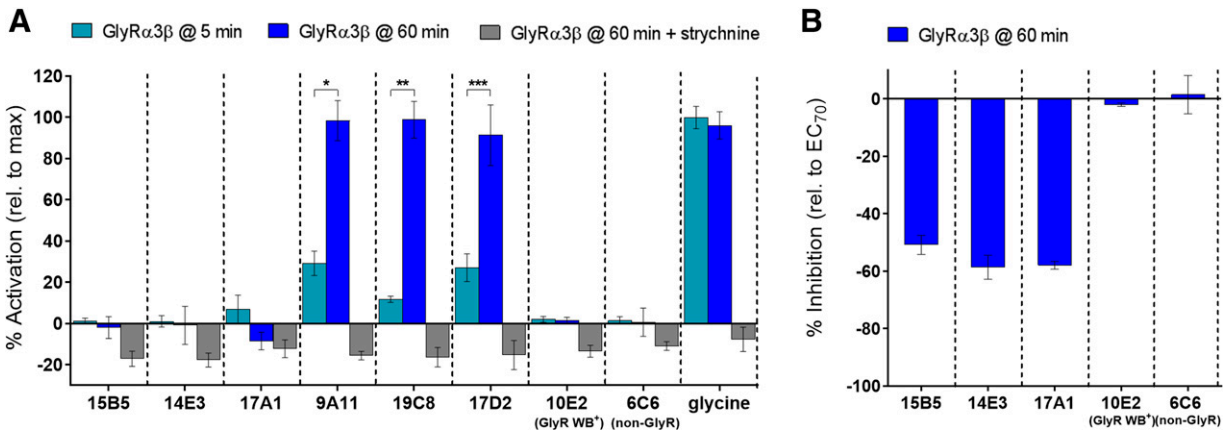

Fig. 1. In vitro functional characterization of anti-GlyR mouse monoclonal antibodies in the MP dye FLIPR assay on human GlyRα3β expressing cell line. Antibodies were first evaluated for agonist-like activity. (A) Activation relative to the maximum achievable glycine response (175 μM glycine) was time-dependent. Three of the eight mAbs tested (9A11, 19C8, 17D2) activated human GlyRα3β in the absence of the agonist glycine within a 5-minute incubation period (light blue bars). This activation was time-dependent, increasing significantly (>99.5% confidence) over a period of 60 minutes (*$t(5) = 14.6$, $p = 0.000027$ for 9A11; **$t(5) = 23.5$, $p = 0.0000026$ for 19C8; ***$t(2) = 19.7$, $p = 0.0026$ for 17D2) (dark blue bars). By contrast, full activation achieved by high concentrations of glycine is achieved within 5 minutes and maintained over the course of 60 minutes. Activation was completely blocked in the presence of 10 μM strychnine (gray bars). (B) Nonactivating GlyR antibodies were assessed for inhibitory activity by adding EC_{70} glycine. Monoclonal Abs 15B5, 14E3, 17A1 were confirmed inhibitors on human GlyRα3β cells. Negative controls included antibody clone 6C6, raised against a membrane transporter unrelated to GlyRs, and anti-GlyRα3 antibody clone 10E2 known to specifically recognize a linear GlyRα3 subunit epitope and used as a western blot (WB) reagent for detection of denatured GlyRα3. Negative controls did not display any functional activity. Glycine alone (175 μM) was used as a positive control, and its response was not time-dependent and was inhibited by strychnine (10 μM). Data represent the mean ± S.D. of data collected in ≥3 independent experiments.

(10 μM) along with each antibody. The slower binding kinetics of antibodies relative to strychnine ensures rapid blockade of all GlyRs present under these assay conditions.

FLIPR kinetic traces were processed using an area under the curve relative to baseline algorithm, where the baseline was the first 10 seconds of the measurement prior to addition of glycine to the cell plate. To examine glycine dose response curves obtained in the presence of fixed monoclonal antibody concentrations, data collected over a period of 60 minutes were subsequently normalized to percent of control (POC) using the maximum achievable glycine response and buffer alone as the assay range references. To determine the functional response of the antibodies, data were subsequently normalized to POC using the maximum achievable glycine response and baseline EC_{10} glycine response as the range references. All POC normalized data were then plotted against log [glycine] or log [antibody], according to the experiment performed, and the data were fit to a nonlinear regression 4-parameter Hill fit to determine the EC_{50} from the resulting sigmoidal curve. Herein, this resulting EC_{50} is defined as the qualitative potency of the antibodies under the in vitro conditions tested. All curve fitting was performed with GraphPad Prism 6 software. For responses collected at 5 and 60 minutes from the same samples, data were graphed as mean ± S.D. and compared using a two-tailed, paired, two-sample equal variance t test. All other comparisons were made using a two-tailed, unpaired, two-sample unequal variance t test and reported as follows: t (degrees of freedom) = t-statistic, p-value).

Immunocytofluorescence. Stable cell lines used for this assay included HEK293T cells overexpressing human GlyRα3β or GlyRα1β or GlyR-free parental control. Cells were plated at a density of 50,000/cells per well in 8-well CC2 treated chamber slides (Nunc, Laboratory Tek II; Sigma-Aldrich) and allowed to grow and expand for 48 hours (37°C, 5% v/v CO_2, and 95% humidity). Full-length primary mouse monoclonal antibodies (mAb 9A11, 14E3, and 19C8) were diluted (@2.5 μg/ml; final concentration) directly into the growth media (see details in *Generation of Stable Human GlyR Cell Lines* section above) and incubated using a standard "live" protocol for 1 hour at 4°C to assess surface binding and selectivity profiles (while minimizing receptor internalization) and washed with cold PBS prior to immediate fixation in fresh 4% paraformaldehyde/PBS (10 minutes). Post live-fixed cells were then rinsed three times in PBS, followed by a 1-hour incubation in the presence of Alexa Fluor-488/goat-anti-mouse-IgG (H+L) secondary antibody (highly cross-absorbed), (Molecular Probes; Thermo Fisher) diluted (1:500) in 5% normal goat serum (NGS)/PBS. Finally, cells were rinsed three more times in PBS and mounted in Fluoroshield media containing dapi staining dye (Sigma-Aldrich), and single plane confocal images were captured on an inverted Carl Zeiss LSM 800 confocal microscope using ZenBlue software (ZEN version 2.1). All steps were performed at room temperature unless otherwise noted.

Antibody Binding by Fluorescence-Activated Cell Sorting. Prior to flow cytometry-based binding experiments, HEK93T human GlyRα3β, GlyRα1β, and parental (GlyR-free) cell lines were treated with 0.25% trypsin-EDTA solution (Gibco, Waltham, MA) and washed with fluorescence-activated cell sorting (FACS) Buffer (BD Biosciences) before addition to 6-well plates. Mouse antibodies at a final concentration of 3 μg/ml were incubated with 1 x 10^6 cells (per well/per condition) on ice for 1 hour, followed by washing with FACS buffer three times to reduce any nonspecific binding. Subsequently, the cells were incubated with the Alexa Fluor-647 labeled anti-mouse secondary antibody (Cell Signaling Technology) on ice for 1 hour, followed by FACS Buffer washing. The collected cells were resuspended in FACS Buffer, and 10 μl of 7-AAD viability dye (BD Biosciences) was added 5 minutes before cell analysis on a BD LSR II flow cytometer (BD Biosciences).

Surface Plasmon Resonance Binding Experiments. To characterize the binding of GlyR antibodies and FAbs to purified GlyR channels, we used surface plasmon resonance (SPR) methods described previously (Huang et al., 2015, 2017). Briefly, SPR spectroscopy measurements were performed on a Biacore T200 (GE Healthcare) at 25°C using PBS pH 7.4 with 1 mM glycine as running buffer. L1 chips were preconditioned with three 30-second injections of 20 mM 3-[(3-cholamidopropyl)dimethylammonio]-1-propanesulfonic acid (CHAPS). Purified human GlyRα3 and GlyRα1 protein were each diluted to 30 μg/ml in PBS pH 7.4 containing 1 mM DDM and 0.1 mg/ml 1-palmitoyl-2-oleoyl-sn-glycero-3-phospho-(1'-rac-glycerol). The protein was passed over L1 chip and adsorbed onto the biosensor at a density of 300–500 Response Units. Lipid solution (i.e., no GlyR) was used as the L1 chip blocking reagent and injected across all flow cells, including reference cell. Using single cycle kinetics method, five sequential injections of increasing concentrations of FAb (i.e., 6.2 nM, 18.5 nM, 55.6 nM, 166.67 nM, and 500 nM) were performed at a flow rate of 50 μl/min.

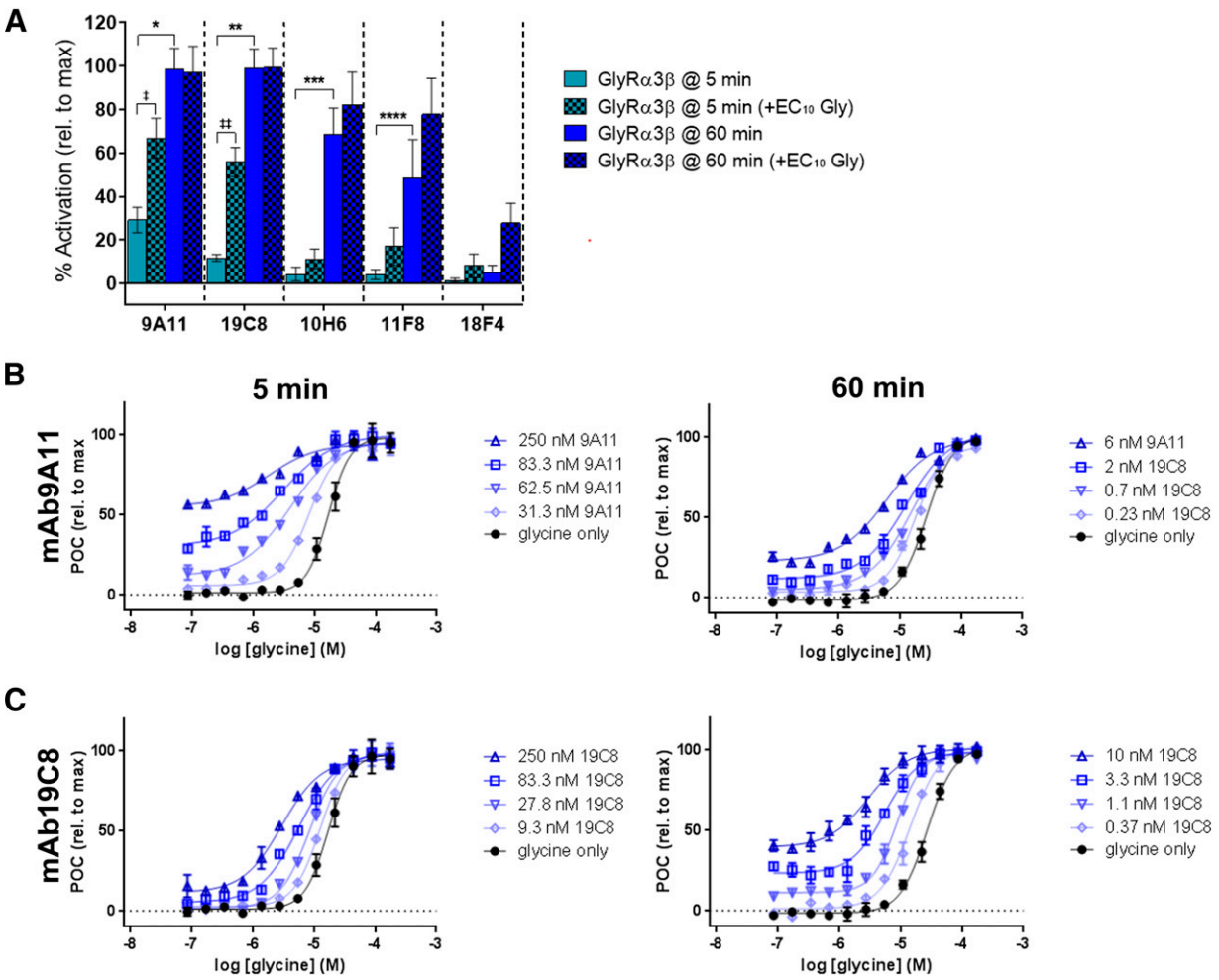

Fig. 2. Functional activation of human GlyRα3β expressing cell line by anti-GlyRα3 mouse monoclonal antibodies is enhanced by the agonist glycine. Potentiation profile of anti-GlyRα3 mAbs that failed the activation screen were further evaluated. (A) Potent anti-GlyRα3 mAbs 9A11 and 19C8 activated human GlyRα3β in the absence of the agonist glycine within a 5-minute incubation period (light blue bars), and the effect increased significantly (>99.5% confidence) over a period of 60 minutes (*$t(5) = 14.6$, $p = 0.000027$ for 9A11; **$t(5) = 23.5$, $p = 0.0000026$ for 19C8) to a level comparable to the maximum achievable glycine response (175 μM glycine). Although the addition of EC_{10} glycine did not further enhance the response at 60 minutes, activation of GlyRα3β by both 9A11 and 19C8 was significantly enhanced (>99.8% confidence) at 5 minutes in the presence of EC_{10} glycine ($^{‡}t(4) = 7.5$, $p = 0.0017$ for 9A11; $^{‡‡}t(3) = 13.0$, $p = 0.00098$ for 19C8). In the absence of glycine, activation of GlyRα3β by anti-GlyRα3 mAbs 10H6 and 11F8 was minimal (<5%) after 5 minutes but increased significantly (>95% confidence) over a period of 60 minutes (***$t(2) = 7.7$, $p = 0.016$ for 10H6; ****$t(2) = 6.1$, $p = 0.025$ for 11F8) reaching ~75%–80% relative to maximum glycine activation. Addition of EC_{10} glycine enhanced response of mAbs 10H6 and 11F8 but was not statistically significant. mAb 18F4 required both EC_{10} glycine and a period of 60 minutes to show any detectable activation response. Data represent the mean ± S.D. of data collected in at least three independent experiments. (B, C) GlyRα3β activator mAbs 9A11 and 19C8 enhanced the potency of the agonist glycine in dose-dependent and time-dependent manner. Both 9A11 and 19C8 mAbs were able to left-shift the glycine dose response curve within 5 minutes (graphs on the left) of addition to cells expressing human GlyRα3β. Comparable effects on glycine potency were achieved with ~40-fold and 20-fold lower anti-GlyRα3 mAb concentrations after 60 minutes for 9A11 and 19C8, respectively (graphs on the right). All data were fit to the mean ± S.D. of responses measured in at least three independent experiments.

Association time was set to 1 minute and final dissociation time to 30 minutes. The binding experiments were performed with 1 mM glycine in PBS pH 7.4 (agonist bound, active channel conformation), and with 1 μM strychnine in PBS pH 7.4 (antagonist bound, resting channel conformation). The raw data were processed using Biacore T200 evaluation software (GE Healthcare) and the data kinetically fit to a 1:1 binding model that included a mass transfer limitation term. Binding experiments were performed in duplicate to calculate the mean association and dissociation rate constants (k_{on} and k_{off}, respectively) and the equilibrium constant (K_d) values (± S.D.).

Tissue Distribution and Open Field Locomotor Activity in Rats. All in vivo procedures described in this manuscript were approved by the Institutional Animal Care and Use Committee at Amgen (IACUC, Thousand Oaks, CA). To compare the brain distribution and subsequent CNS-related effects of therapeutic positive modulators of GlyRs, the two strongest antibodies were chosen, described herein: mAbs 9A11 and 19C8. In brief, adult male Sprague Dawley rats (250–350 g, 8–12 weeks old, Charles River Laboratories, Hollister, CA) were intravenously dosed with 9A11 or 19C8 (10, 30, or 100 mg/kg) or a non-targeting isotype control (IgG1 or IgG2a) in 10 mM sodium acetate (9% sucrose, pH 5.2), immediately placed into low-light open-field chambers (Kinder Scientific, San Diego, CA), and monitored for basic movements and rearing over a 30 minute observation period using an automated infrared photobeam approach. Open-field data were assessed using a one-way ANOVA to assess the overall test article treatment effect followed by Dunnett's multiple comparison post hoc tests (GraphPad Prism 5; GraphPad Software Inc., La Jolla, CA).

At 30 minutes post dose, a blood sample was collected via tail vein sampling and processed to obtain serum for subsequent bioanalysis. Rats were then placed under 5% isoflurane anesthesia to allow for a transcardiac saline perfusion followed by a craniotomy to collect whole brain samples. The perfused brain tissue was rinsed, weighed, and

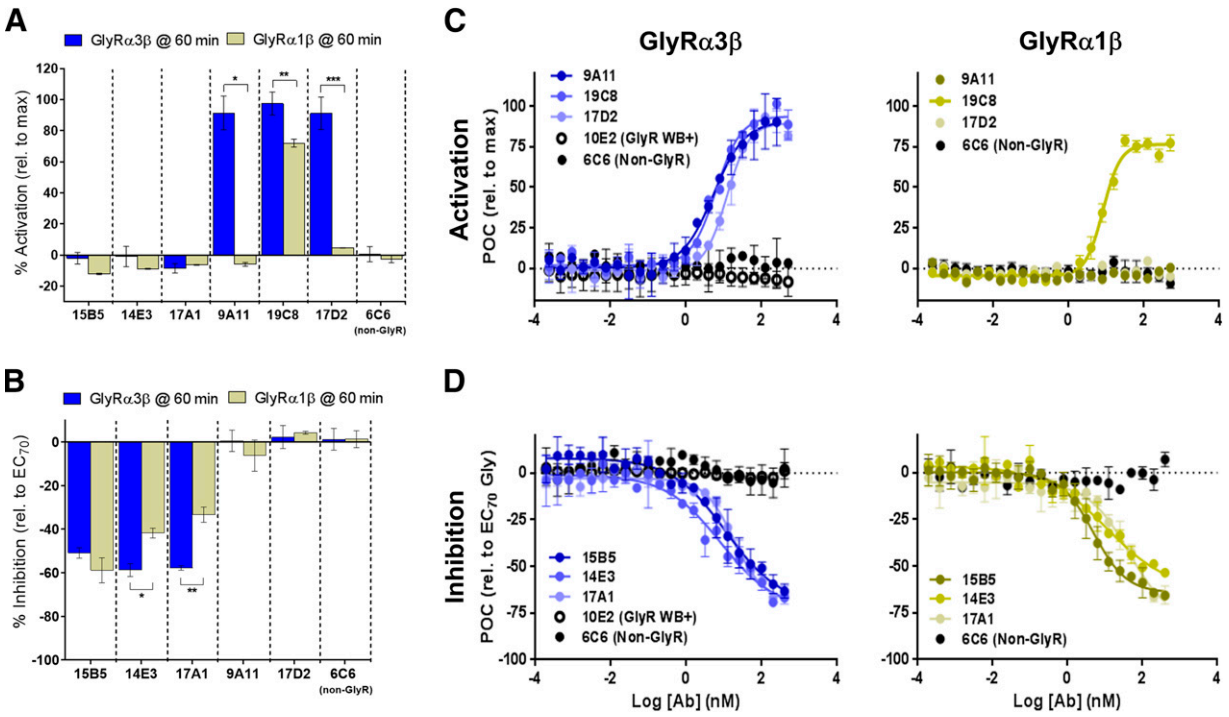

Fig. 3. Selectivity and activity assessments of mean functional response of anti-GlyRα3 monoclonal antibodies on human GlyRα3β or GlyRα1β expressing cell lines. (A) Selectivity of activation was assessed following a 60-minute incubation of cells expressing human GlyRα3β (blue) or GlyRα1β (yellow) with each mAb (100 nM). Responses were compared with the maximum achievable glycine response (175 μM glycine) over the same time period. Monoclonal Abs 9A11 and 17D2 produced activation profiles that were significantly different (>99.5% confidence) between cells expressing GlyRα3β (>90%) and GlyRα1β (<5%) after 60 minutes (*$t(2) = 15.4$, $p = 0.0042$ for 9A11; ***$t(2) = 14.4$, $p = 0.0048$ for 19C8) and demonstrated a high degree of selectivity for GlyRα3β. Monoclonal Ab 19C8 also produced significantly different responses (>95% confidence) but demonstrated a poorer overall selectivity profile by activating both channel subtypes >70% (**$t(2) = 5.6$, $p = 0.030$ for 19C8). Negative controls mAb 6C6 and 10E2 had no functional activity on either cell line. (B) Selectivity of inhibition of human GlyRα3β and GlyRα1β receptors was assessed by subsequently adding EC_{70} glycine. There was no significant difference observed between GlyRα3β (>50% inhibition) and GlyRα1β (>55% inhibition) expressing cells for mAb 15B5. Monoclonal Abs 14E3 and 17A1 produced significantly different (>99% confidence) responses between cell lines while displaying preferential inhibition of GlyRα3β (*$t(4) = 7.9$, $p = 0.0014$ for 14E3; **$t(2) = 11.6$, $p = 0.0074$ for 17A1). Monoclonal Abs 14E3 and 17A1 demonstrated poor overall selectivity by inhibiting both GlyRα3β and GlyRα1β >35%. (C) Dose response activation curves for mAb 9A11, 19C8, 17D2, 15B5, 14E3, and 17A1 were obtained after a 60-minute incubation in the absence of glycine with cells expressing human GlyRα3β (left panel in blues) or GlyRα1β (right panel in yellows). (D) Dose response inhibition curves were obtained in the presence of EC_{70} glycine with cells expressing human GlyRα3β (left panel in blues) or GlyRα1β (right panel in yellows). All data were fit to the mean ± S.D. of responses measured in at least three independent dose response experiments.

homogenized prior to bioanalysis. Concentrations of the antibodies in whole brain homogenate were assumed to be indicative of concentrations at the pharmacological site of action, and more definitive imaging or microdialysis studies were not conducted. Concentrations of mAbs 9A11, 19C8, or the isotype controls were measured in the resulting serum and brain samples using an anti-mouse IgG immunoassay on the MSD platform (Meso Scale Discovery, Rockville, MD). Capture and detection reagents consisted of a biotinylated anti-mouse IgG antibody and sulfo-tagged goat anti-mouse IgG1 or IgG2a antibody, respectively. Standard curves were included for all analytes in each respective matrix and used to extrapolate final analyte concentrations. As exploratory pharmacokinetic/tissue distribution studies with mAbs 9A11 and 19C8 demonstrated typical antibody pharmacokinetic profiles (Supplemental Fig. 1) and spinal cord exposures that were equal to or greater than those observed in the brain (Supplemental Fig. 2), only whole brain tissue was collected from the open-field locomotor studies and used as a surrogate for both tissue types.

Results

1. Functional Characterization & Selectivity of GlyRα3 Monoclonal Antibodies. A panel of 6 full-length mouse monoclonal antibodies (mAbs) and corresponding fragment antigen binding (FAbs) antibodies generated against human GlyRα3 was evaluated in an in vitro cell-based assay to assess their ability to modulate human GlyR activity. The functional assays employed HEK293T cell lines overexpressing either homomeric or heteromeric subtypes of human GlyRs (GlyRα1, GlyRα3, GlyRα1β, GlyRα3β). A MP dye added to the cells reported on net changes in membrane potential induced by the addition of a single fixed concentration of antibody (100 nM) or high concentration of the endogenous agonist glycine (175 μM; positive control) over time. In the absence of the agonist glycine, mAbs 9A11, 19C8, and 17D2 (Fig. 1A, light and dark blue bars) were found to activate human GlyRα3β in a time-dependent manner and were also able to achieve maximal fluorescence responses comparable to those induced by high concentrations of glycine alone but in a slower time frame. For mAbs 9A11, 19C8, and 17D2, the extent of activation increased significantly over time and reached a maximal level, comparable to that induced by high concentrations of glycine alone, within 60 minutes (dark blue bars). All antibodies tested were fully inhibited in the presence of the potent GlyR antagonist strychnine (10 μM) (Fig. 1A, gray bars) demonstrating the on-target activation of the channel and suggesting that antibody-mediated GlyRα3β activation is a reversible process. Conversely, mAbs 15B5, 14E3, and 17A1 showed no time-dependent activation of GlyRα3β within

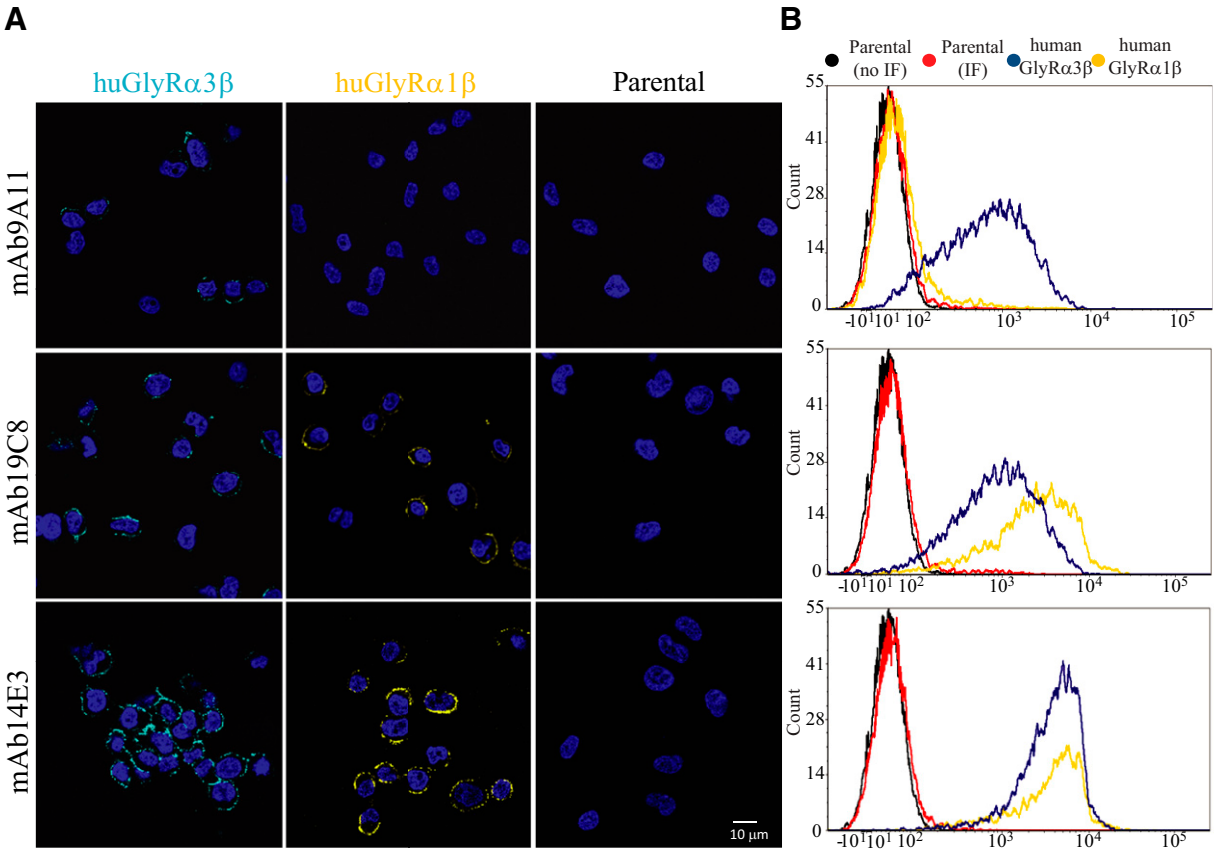

Fig. 4. Cell surface binding of anti-GlyR mouse monoclonal antibodies to human GlyR$\alpha 3\beta$ or GlyR$\alpha 1\beta$ cell lines. The cell surface binding patterns of mAbs to three separate HEK293T cell lines expressing GlyR$\alpha 3\beta$ (blue), GlyR$\alpha 1\beta$ (yellow), or GlyR-free parental were assessed using immunocytofluorescence (ICF) (A) and FACS (B). (A) Representative photomicrographs using GlyR$\alpha 3$ mAb 9A11 and 14E3 and 19C8 in live cells confirmed that mAb 9A11 selectively recognized cells expressing human GlyR$\alpha 3\beta$, whereas mAbs 14E3 and 19C8 recognized both GlyR$\alpha 3\beta$ and GlyR$\alpha 1\beta$ cell lines. Parental HEK293T cells were used as a negative control and were not labeled by any of the mAbs tested herein. (B) Representative FACS traces of live HEK293T cells used in the ICF study further confirmed the same cell surface binding patterns. (Scale bar = 10 μm).

the 60-minute incubation period. However, subsequent addition of glycine (equal to the GlyR$\alpha 3\beta$ EC_{70} for glycine) to these cells revealed that these three antibodies significantly blocked the glycine-induced fluorescence response, suggesting that these mAbs are negative modulators of GlyR$\alpha 3\beta$ (Fig. 1B, dark blue bars), as opposed to the first three that displayed a time-dependent agonist-like profile. The negative controls included monoclonal antibody 10E2 (an anti-GlyR$\alpha 3$ antibody, generated during the antibody campaign, that was able to recognize a linearized epitope and was used for western blotting only) and mAb 6C6 (a mouse monoclonal antibody against another non-GlyR membrane transporter and therefore does not recognize GlyRs). Neither of these negative controls (mAbs 10E2 and 6C6) were found to modulate the response of GlyR$\alpha 3\beta$ (Fig. 1, A and B).

Next, we investigated the ability of the agonist glycine to enhance positive modulation of GlyR$\alpha 3\beta$ by lower affinity mAbs (mAbs 10H6 and 11F8) that showed a statistically significant activation profile in the absence of glycine (Fig. 2A). However, mAbs 10H6 and 11F8 could only achieve a partial response (75%–80% of max glycine response) compared with the more active mAbs 9A11 and 19C8 over the same 60-minute period. We found that the addition of a low concentration of glycine (equal to the EC_{10} for each of the channels expressed) resulted in a consistent, but not statistically significant, enhancement of GlyR$\alpha 3\beta$ activation by mAbs 10H6 and 11F8 at both 5- and 60-minute timepoints. Lastly, the weakest mAb tested (18F4) required both EC_{10} glycine and a period of 60 minutes to show a detectable GlyR$\alpha 3\beta$ activation response. To better understand the interplay between glycine and the positive modulator antibodies on GlyR$\alpha 3\beta$, we also measured glycine potency in the presence of increasing concentrations of the most active positive modulators: mAb 9A11 and 19C8 (i.e., Schild Shift assay). We found that these antibodies increased glycine potency in both a dose- and time-dependent manner but did not modulate the efficacy of the agonist glycine (Fig. 2, B and C).

To further assess for α subunit selectivity within the GlyR receptor family, all mAbs were tested against human GlyR$\alpha 1\beta$ stably expressing HEK293T cells, the most relevant and complementary glycine channel subtype. In the absence of the endogenous ligand glycine, mAb 19C8 was found to stimulate GlyR$\alpha 1\beta$ in a time-dependent manner (data not shown) and in a way that was approaching near maximal fluorescence response comparable to that induced by high concentrations of glycine alone within 60 minutes of incubation (Fig. 3A, yellow bars). Interestingly, positive modulator mAbs 9A11 and 17D2 did not appear to activate GlyR$\alpha 1\beta$ within the same timeframe, a significant difference from the responses observed in GlyR$\alpha 3\beta$ expressing cells, suggesting that mAb 9A11 and 17D2 are highly selective for GlyR$\alpha 3\beta$ over GlyR$\alpha 1\beta$ under these assay conditions. Similarly,

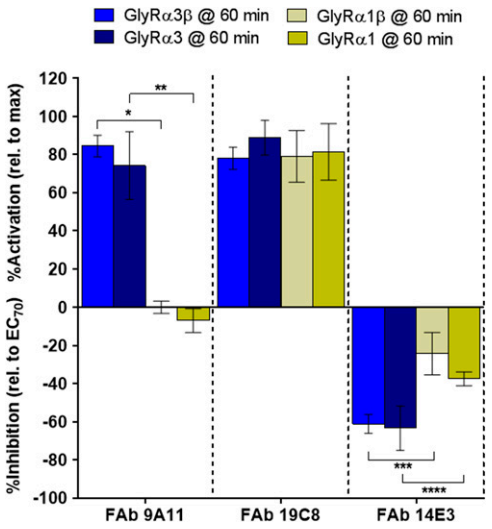

Fig. 5. Characterization of mean functional response of FAbs generated from mAb 9A11, 19C8, and 14E3 on human GlyRα3(β) or GlyRα1(β) cell lines. Activation of GlyRα3(β) (blues) and GlyRα1(β) (yellows) expressing cells was assessed relative to the maximum achievable glycine response (175 μM glycine) after 60 minutes incubation with 100 nM fixed concentration of each FAb. FAb 9A11 produced activation profiles that were significantly different (>99.9% confidence) between cells expressing GlyRα3(β) (75%–85%) and GlyRα1(β) (<5%) after 60 minutes (*$t(4)$ = 29.8, p = 0.0000075 for GlyRα3β versus GlyRα1β; **$t(2)$ = 7.5, p = 0.017 for GlyRα3 versus GlyRα1) and demonstrate a high degree of selectivity for GlyRα3(β) channels, which is consistent with the FLIPR and ICF/FACS data. FAb 19C8 was nonselective and positively modulated all tested GlyR channels similarly. Inhibition by nonactivating FAbs was further assessed by adding EC_{70} glycine. The FAb 14E3 produced significantly different (>95% confidence) responses between cell lines while displaying preferential inhibition of GlyRα3(β) (***$t(6)$ = 6.4, p = 0.00068 for GlyRα3β versus GlyRα1β; ****$t(2)$ = 5.2, p = 0.035 for GlyRα3 versus GlyRα1). FAb 14E3 demonstrated poor overall selectivity by inhibiting all GlyRα3β and GlyRα1β subtypes >25%. FAb 14E3 inhibited all channels and displayed an apparent preference for negative modulation of GlyRα3(β) over that of GlyRα1(β). Data represent the mean ± S.D. of data collected in at least three independent experiments.

to what is shown in Fig. 1, mAbs 15B5, 14E3, and 17A1 did not activate the GlyRα1β channel within the incubation period tested. To further interrogate the function and affinity of these mAbs, we examined their ability to either potentiate or block the GlyRα1β channel activation by subsequent addition of glycine (equal to the GlyRα1β EC_{70} for glycine) (Fig. 3B, yellow bars). Upon subsequent addition of EC_{70} glycine, mAbs 15B5, 14E3, and 17A1 blocked the resulting fluorescence response in each cell line, analogous to the GlyR antagonist strychnine (data not shown). There was no significant difference observed between GlyRα3β (>50% inhibition) and GlyRα1β (>55% inhibition) expressing cells for mAb 15B5. Interestingly, mAbs 14E3 and 17A1 produced significantly different responses in GlyRα3β or GlyRα1β expressing cells but inhibited responses of both channel subtypes by 35%–58%, suggesting that they act as nonselective negative modulators of human GlyRs.

After this initial assessment of function and selectivity, we selected the positive and negative modulator mAbs, which induced the strongest responses and used the MP dye assay to determine their EC_{50} or IC_{50}, respectively, on the human GlyRα3β and GlyRα1β cell lines. These included: mAbs 9A11, 19C8, and 17D2 (as positive modulators) and 15B5, 14E3, and 17A1 (as negative modulators). Positive modulator antibody strength was determined by measuring the fluorescence response in the absence of glycine, whereas that of negative modulator antibody was measured upon subsequent addition of EC_{70} glycine. All antibodies modulated GlyR activity in the low nM range (see Table 1). The three identified positive modulators (mAbs 9A11, 19C8, and 17D2) reached a maximal (>90%) activation level comparable to high concentrations of glycine (Fig. 3C) and activated with EC_{50}s in the 5–12 nM range on the human GlyR heteropentamer cell lines (Table 1). The GlyRα3-selective positive modulators mAb 9A11 and 17D2 showed no functional activity on GlyRα1β, whereas the nonselective mAb 19C8 activated GlyRα1β (Fig. 3C) with a comparable EC_{50} of 9 nM, as observed for GlyRα3β (Table 1). The three identified nonselective negative modulators reached a maximal inhibition level of 60%–70% (Fig. 3D) with IC_{50} values in the 8–20 nM range on GlyRα3β (Table 1) and a maximal inhibition level of 55%–65% on GlyRα1β (Fig. 3D) with IC_{50} values in the 5–45 nM range (Table 1).

To complement the functional data and to further characterize the selectivity profiles of the monoclonal antibodies identified, we used two independent techniques to visualize and confirm the cell surface binding patterns of the strongest mAbs from each functional category: mAb9A11 – selective positive human GlyRα3 modulator; mAb19C8 – nonselective positive modulator; mAb14E3 – nonselective negative modulator of cells overexpressing human GlyRα3β or GlyRα1β. Using immunocytofluorescence, we detected cell surface labeling on both cell lines for nonselective mAbs 19C8 and 14E3, whereas the functionally selective mAb 9A11 labeled human GlyRα3β expressing cells only, in agreement with our functional data (Fig. 4A). In addition, the cell-surface binding of these antibodies was further examined using flow cytometry as a complementary platform (Fig. 4B). In accordance with the previous data, mAb 9A11 was the only antibody that showed a selectivity profile of human GlyRα3β over GlyRα1β. Parental GlyR-free HEK293T cells were used as a negative control in both fluorescence-based platforms, and no binding was detected (Fig. 4, A and B). The immunofluorescent assays performed herein were purposefully done at 4°C to minimize surface receptor internalization to support the characterization goal of confirming their cell surface selectivity profiles. These assays do not address the GlyR internalization potential of the antibodies. Such studies would need to be performed at room temperature. Together, these complementary results further support and strongly correlate with the selectivity profiles reported in the functional assay and suggest that mAb 9A11 is a selective GlyRα3β functional monoclonal antibody.

2. Biophysical Characterization of Fragmented Monoclonal Antibodies. To further understand the mechanisms underlying the selectivity and functional profile of these antibodies, we characterized the binding of mAb 9A11, 19C8, and 14E3 onto purified human GlyRα1 and α3 homopentameric ion channel proteins using SPR (purified heteropentamer material did not yield in sufficient amounts). Due to technical limitations in the method related to the bivalency of a full-length mAbs, all binding characterizations were completed using monovalent fragments (FAbs) of each respective antibody (9A11, 19C8, and 14E3). Therefore, we first characterized each FAb in the functional assay to determine their functional and selectivity profile as well as the activity profiles. To make direct comparisons with the channel subtypes available to us for SPR binding studies (homopentameric only), we extended the functional assay assessment of FAbs 9A11, 19C8, and 14E3 to include two additional HEK293T cell

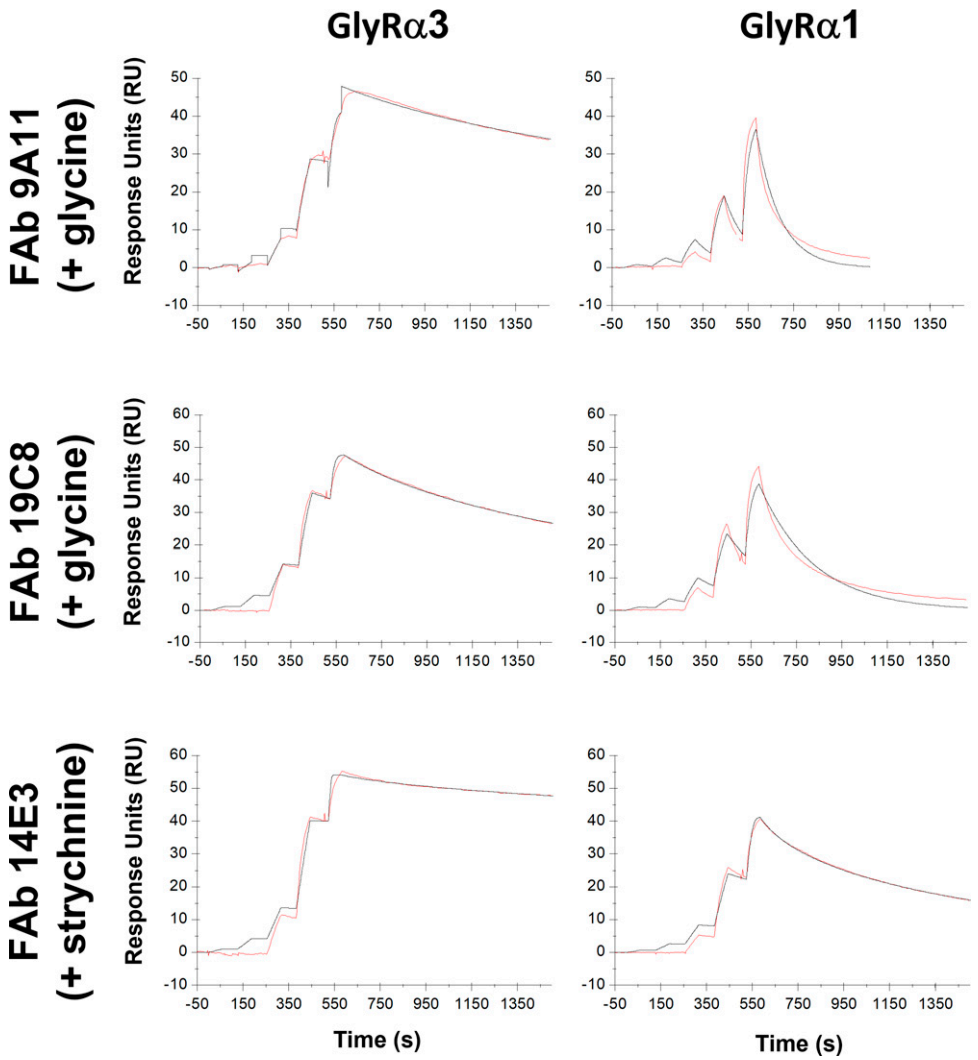

Fig. 6. Representative SPR binding kinetic traces for the binding of FAbs 9A11, 19C8, and 14E3 to purified human GlyRα3 and GlyRα1 channel protein. All FAbs were tested in the presence of 1 mM glycine or 1 μM strychnine to induce the active or resting conformation of the GlyR channels, respectively. FAb 14E3 bound with highest affinity to the resting channel conformation, whereas FAb 19C8 bound with highest affinity to the active channel conformation. Black traces reflect the observed binding data from sequential injections of increasing concentrations of FAb (6.2nM, 18.5nM, 55.6nM, 166.67nM, and 500nM). Red traces reflect a data fit to a 1:1 binding model. FAb 9A11 bound with comparable affinities to both channel conformations. All three FAbs showed varying preferences for GlyRα3 in the SPR binding assay due to slower dissociation rates from that channel. FAb 9A11 was the most α3-selective FAb in our collection.

lines expressing either homopentameric human GlyRα3 or GlyRα1, each lacking the β subunit.

In the absence of the endogenous ligand glycine, FAb 9A11 triggered significantly different activating responses in cells expressing GlyR$\alpha3\beta$ or GlyRα3 when compared with GlyR$\alpha1\beta$ or GlyRα1, which were unresponsive during the 60-minute incubation period. These findings confirm that the FAb 9A11 retained the highly GlyRα3-selective activation profile of the full-length 9A11 mAb. Similar to full-length mAb 19C8, FAb 19C8 was found to stimulate all four GlyR cell lines comparably. Both reached the maximal fluorescence response (100%) analogous to that induced by high concentrations of glycine alone (Fig. 5). FAb 14E3 blocked the fluorescence response induced by the addition of glycine (equal to the glycine EC_{70} for each respective channel), suggesting that this FAb functioned as a negative modulator of all GlyR channels. Although FAb 14E3 produced significantly different responses in cells expressing GlyR$\alpha3(\beta)$ (61%–64% inhibition) and GlyR$\alpha1(\beta)$ (24%–37%), the selectivity profile across all four cell lines is less robust, since there is appreciable activity across all channel subtypes. Together, this characterization aligns with the corresponding functional profiles described using the full-length mAbs in the same assay and highlights the alignment of the data obtained on the heteropentameric and the corresponding homomeric human cell lines. Interestingly, each full-length mAb was 3- to 5-fold more active than each corresponding FAb (Table 1). This is not necessarily surprising considering that each full-length mAb is bivalent and may be able to interact with multiple GlyR subunits at the same time. Nevertheless, the functional and selectivity profiles for all three FAbs correlate well with those observed for the full-length mAbs originally tested against GlyR$\alpha3\beta$ and GlyR$\alpha1\beta$ (see Fig. 3; Table 1).

After confirming that each FAb retained the functional and selectivity profiles of the full-length mAbs, we followed with the intended SPR studies on purified human GlyRα3 and GlyRα1 homopentameric ion channels to characterize the kinetic

TABLE 2
Summary of SPR binding kinetic data to purified homopentameric human GlyRα receptors
Values represent mean ± S.D. of at least two independent SPR experiments.

		GlyRα3			GlyRα1		
FAb	**Condition**	**k_{on} ($M^{-1}s^{-1}$)**	**k_{off} (s^{-1})**	**K_d (nM)**	**k_{on} ($M^{-1}s^{-1}$)**	**k_{off} (s^{-1})**	**K_d (nM)**
14E3	+ glycine	$5 \pm 3 \times 10^5$	$3 \pm 2 \times 10^{-2}$	53 ± 14	$2.2 \pm 0.6 \times 10^4$	$1.7 \pm 0.3 \times 10^{-2}$	803 ± 155
	+ strychnine	$10 \pm 2 \times 10^5$	$< 1 \times 10^{-5}$	< 0.3	$2.4 \pm 0.3 \times 10^5$	$2.6 \pm 0.5 \times 10^{-3}$	11 ± 3
19C8	+ glycine	$1.6 \pm 0.5 \times 10^5$	$7 \pm 3 \times 10^{-4}$	5.0	$7 \pm 1 \times 10^4$	$4.5 \pm 0.8 \times 10^{-3}$	63 ± 19
	+ strychnine	$6 \pm 2 \times 10^4$	$1.8 \pm 0.5 \times 10^{-3}$	29 ± 6	$7.1 \pm 0.3 \times 10^4$	$1.2 \pm 0.3 \times 10^{-2}$	169 ± 50
9A11	+ glycine	$1.9 \pm 0.4 \times 10^5$	$7 \pm 2 \times 10^{-4}$	3.7 ± 0.6	$7 \pm 2 \times 10^4$	$8 \pm 2 \times 10^{-3}$	129 ± 44
	+ strychnine	$1.0 \pm 0.3 \times 10^5$	$8 \pm 5 \times 10^{-4}$	8 ± 3	$6 \pm 2 \times 10^4$	$10 \pm 2 \times 10^{-3}$	180 ± 58

parameters (k_{on}; k_{off}) that contribute to FAb affinity (K_d). To probe the relationship between binding affinity and channel conformation, these studies were carried out in the presence of agonist glycine (active channel conformation) or antagonist strychnine (predominantly resting channel conformation). FAb 9A11 was found to be functional in the cell-based assays and positively modulated the activity of only GlyRα3(β) channels. SPR binding studies found that FAb 9A11 had 30–40X higher affinity for GlyRα3 when compared with GlyRα1, consistent with the activity profile. The higher affinity for GlyRα3 is due primarily to a significantly slower off-rate from GlyRα3 relative to GlyRα1 (Fig. 6, top row). FAb 9A11 binds the active and resting conformations of the purified GlyRα3 with comparable affinities but shows a 2- to 3-fold higher preference for the active conformation (Table 2). Interestingly, FAb 19C8 is nonselective in the functional assays but binds with 15-fold higher affinity for purified GlyRα3, which appears to be mostly due to a reduced k_{off} relative to GlyRα1 (Fig. 6, middle row). When tested in the presence of glycine or strychnine, the positive modulator FAb 19C8 has a 4–6X higher affinity preference for active GlyR channel conformation (Table 2). In contrast, the negative modulator FAb 14E3 binds the resting conformation of both GlyRα channels with 80–100X higher affinity over the active channel conformation, which agrees with the inhibitory function of this FAb in cell-based assays (Fig. 6, bottom row; Table 2). In the strychnine-bound channels, this nonselective FAb appears to bind with a 15X higher affinity to purified GlyRα3, which might be caused by a reduced k_{off} relative to GlyRα1. Based on the complete biophysical characterization of FAb 9A11, an affinity difference of >30-fold between two different channels may be required to reflect an in vitro selectivity profile from a functional standpoint. However, the relevance of these numbers in vivo has yet to be determined.

3. In Vivo Assessment of Tissue Distribution and Effect on General Locomotor Activity. To enable subsequent in vivo studies in rats, it was necessary to first evaluate HEK293T cells transiently expressing homomeric rat GlyRα3 and GlyRα1 using the same set of mAbs and FAbs to guide in the proper dosing range required for target engagement. Due to the transient nature of the expression of the rat channel, combined with the observation that the tool-reagents behave similarly on the homopentameric and heteropentameric channel compositions, we limited the scope of the in vivo study to GlyR homopentamers. We found that the affinities and selectivity profiles were highly consistent across species (selective activation by 9A11, rat-GlyRα3/rat-GlyRα1: 43 nM/no binding; nonselective activation by 19C8, ratGlyRα3/ratGlyRα1: 15.6 nM/47.0 nM).

In an effort to determine the impact of GlyRα-selectivity on the overall behavior in vivo, we selected an optimal pair of positive modulators from our collection: mAb 9A11 (GlyRα3 selective) and 19C8 (GlyRα3/1). After a single intravenous administration of the selected antibodies across a dose range of 10, 30, and 100 mg/kg, the serum exposure of mAbs 9A11 or 19C8 was assessed to ensure both antibodies achieved similar target coverage relative to their in vitro EC_{50} values. A dose-dependent increase was observed across the doses, tested, and resulted in similar serum exposures for 9A11, 19C8, or their respective isotype controls (isotype controls evaluated only at 100 mg/kg; Fig. 7A). Brain exposure was also comparable between mAbs 9A11 and 19C8 and accounted for approximately 0.02%–0.05% of the total intravenous dose with a brain/plasma ratio of 0.4%–0.7% (Fig. 7B). Antibody concentrations in brain homogenate were assumed to be indicative of concentrations at the site of action (Chang et al., 2019). Assessment of target coverage suggests that mAbs 9A11 (GlyRα3) and 19C8 (GlyRα1/3) achieved approximately 1 - to 3-fold coverage of their respective calculated in vitro rat EC_{50} values in brain tissue (Fig. 7C). Based on preliminary pharmacokinetic/tissue distribution studies, spinal cord target coverage for both mAbs would be expected to be equal to or greater than that observed in brain homogenate (Supplemental Fig. 2).

Each test group was monitored for basic movements and rearing from 0–30 minutes postdosing. After the intravenous administration of the GlyRα3/1 mAb 19C8, labored breathing was observed with increased severity with each escalating dose. For ethical reasons, this resulted in all the animals in the 100 mg/kg cohort being taken off-study prior to open field assay (OFA) analysis. Labored breathing was not observed after intravenous administration of the monoclonal GlyRα3-selective antibody 9A11 up to 100 mg/kg, and no adverse effects were observed with either isotype control. In the OFA, the GlyRα3-selective antibody (mAb 9A11) did not significantly alter either measurement at any of the doses tested in the study (Fig. 8A). Conversely, the pan-GlyRα antibody (mAb 19C8) resulted in a statistically significant 58% reduction in rearing counts at 10 mg/kg and a nonstatistically significant reduction of 25% at 30 mg/kg (Fig. 8B) with similar serum and brain exposure. Overall, both the presence of labored breathing and impact on rearing counts suggest that the selective profile of mAb 9A11 is favorable over that of the GlyRα3/1 mAb 19C8 within 10–100 mg/kg dose range.

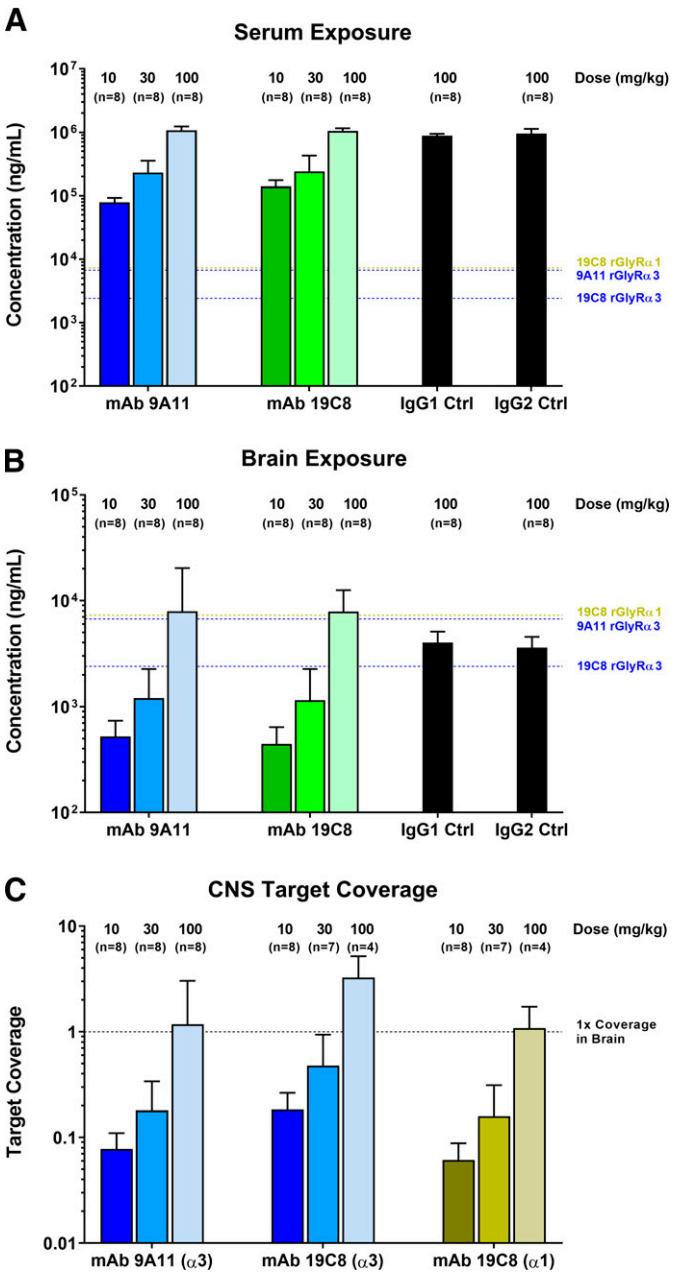

Fig. 7. Dose range finding serum and brain exposure of mAbs 9A11 and 19C8 and corresponding isotype controls after a single intravenous administration in adult male Sprague-Dawley rats. Serum (A) and brain (B) exposures to mAbs 9A11 (selective agonist; blue) and 19C8 (pan-GlyR agonist; green) assessed 30 minutes post dose exhibited a classic dose-dependent increase comparable to the exposure of the isotype control antibodies at 100 mg/kg. The dotted lines represent the corresponding rat (r) GlyRα3 (blue) or GlyRα1 (yellow) channel in vitro EC_{50} values. (C) The resulting brain exposures were of sufficient magnitude to cover by 1– 3-fold their respective measured rat GlyRα3 (blue) and/or GlyRα1 (yellow) in vitro EC_{50} values in the 100 mg/kg dose group.

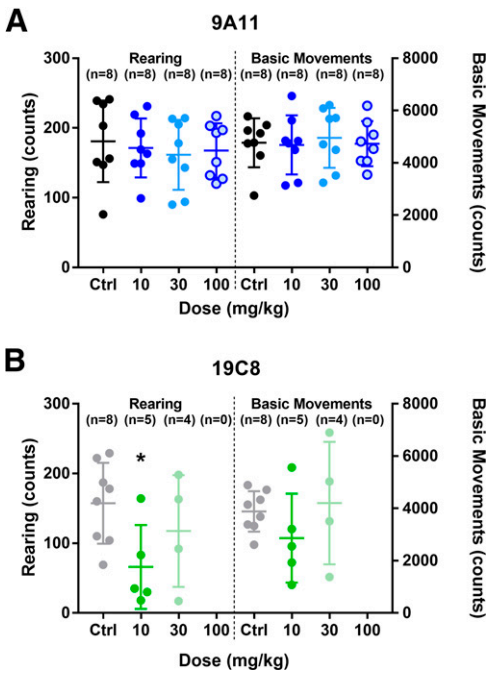

Fig. 8. Open field assessment dose response of mAbs 9A11 and 19C8 after a single intravenous administration in adult male Sprague-Dawley rats. The effects of dosing male Sprague-Dawley rats with mAbs 9A11 (selective agonist; blue) or 19C8 (pan-GlyRα3/1 agonist; green) on general locomotor activity was assessed by unbiased-electronic scoring of total basic movement and total rearing. (A) The GlyRα3-selective mAb 9A11 (blue) did not result in statistically significant changes to either total rearing counts or basic movement over a 30-minute period after intravenous dosing ranging from 10–100 mg/kg. (B) A 58% reduction in total rearing counts [$*P < 0.05$, Dunnett's multiple comparison test (MCT)] was observed after a 10 mg/kg intravenous administration of the pan-GlyRα3/1 mAb 19C8 (green). More importantly, all animals in the 100 mg/kg mAb 19C8 test group were taken off study prior to open-field assessment due to general health observations (labored breathing).

Discussion

Ion channels play a critical role in modulating a variety of cellular functions, making them an important target-class for drug discovery. Although the majority of the efforts revolve around small molecule modalities, monoclonal antibody approaches (mAbs) have been investigated; however, their therapeutic potential remains largely underexploited.

Herein, we present an approach combining an antibody campaign with an HTS platform to identify large molecules capable of modulating the Cys-Loop family of ligand-gated ion channels. By using complementary in vitro approaches (FLIPR, immunocytofluorescence, FACS, and SPR), we identified and characterized selective and pan-surface binding monoclonal antibodies against the alpha subunit of GlyRs and found a strong correlation between observed cell surface binding and functional selectivity (Table 3). We further expended the characterization of selected tool antibodies to in vivo testing by assessing their CNS penetrance and safety profiles and determined that GlyRα3-selective antibody had a larger dosing window and a lower impact on basic motor behaviors after a single intravenous administration.

Given the general complexity and size of ion channels, it is no surprise that generating functional antibodies has shown limited therapeutic success. Some of the difficulties include structural and technical considerations, such as limitations in expressing and purifying full-length human protein and challenges in designing biologically relevant HTS functional assays (reviewed in Wilkinson et al., 2015). In drug research and development, antibodies targeting complex membrane proteins may exhibit similar characteristics to those of small molecules, but their greater potential for selectivity, exquisite specificity, and long plasma half-life can enable optimization of highly desirable and therapeutically relevant attributes,

TABLE 3
Correlation of FLIPR assay functional response with cellular binding determined by immunocytofluorescence against human GlyR expressing cell lines

mAb	Immunocytofluorescence		Functional Profile		Selectivity Profile on GlyRs
	GlyR$\alpha3\beta$	GlyR$\alpha1\beta$	GlyR$\alpha3\beta$	GlyR$\alpha1\beta$	
14E3	++	++	Inhib.	Inhib.	GlyRα3/1
15B2	++	++	Inhib.	Inhib.	GlyRα3/1
17A1	++	++	Inhib.	Inhib.	GlyRα3/1
19C8	++	++	Activ.	Activ.	GlyRα3/1
9A11	++	NB	Activ.	None	GlyRα3
17D2	++	NB	Activ.	None	GlyRα3
6C6	NB	NB	None	None	NB
10E2	NB	NB	None	None	NB

NB, no binding detected.

such as affinity, potency, effector function, and pharmacokinetic property (Dodd et al., 2018). It has yet to be fully understood whether partial crossing of the BBB can be leveraged for such molecules in the presence or absence of a shuttle-protein, but the recent regulatory approval of aducanumab (Aduhelm) is evidence that some antibodies can cross BBB sufficiently. With advancements in the delivery of molecules across the BBB, the extended application of therapeutic antibodies to the CNS might be achieved (reviewed in Gosselet et al., 2021).

It is noteworthy that most of the successful antibody campaigns, including representatives from the following ion-channel families: ligand gated ion channels, voltage-gated channels, calcium release-activated channels, and transient receptor potential channels (Sun and Li, 2013; Wilkinson et al., 2015; Hutchings et al., 2019) resulted in functional target blockers, suggesting that the generation of activating antibodies is a relatively rare event and/or is under-represented in the field due to higher biologic relevance of ion channel blockers. Within the aforementioned list, one will appreciate the near absence of engineered antibodies targeting members of the Cys-Loop family of ligand-gated ion channels. Indeed, glycine receptors play an important role in central inhibition, where positive modulation of these channels leads to neuronal silencing, thus offering a way to modulate various neurologic conditions with underlying neuronal hyperexcitability symptoms. The naturally occurring antagonist-GlyRα1 antibodies reported in adult and pediatric patients suffering from progressive encephalomyelitis with rigidity and myoclonus suggest that this target-class can be modulated by large-molecules, if present in sufficient concentration in the CNS. Moreover, the antagonist profile of those antibodies aggravates the patients' symptoms, thus highlighting a therapeutic need for activators of the corresponding receptors and/or neuronal pathways (see reviews by Sarva et al., 2016; Crisp et al., 2019). The herein described GlyR antibody campaign has given rise to GlyRα-selective monoclonal antibodies with diverse activity modulating profiles (activators and inhibitors).

We further leveraged SPR studies of purified human GlyRα3 and GlyRα1 ion channels to understand the contribution of on and off rates to binding affinities. A closer analysis of the SPR binding data revealed that the selective tool-antibodies showed a clear difference in binding kinetics between the two GlyRα channel subtypes. SPR binding data suggest that i) these antibodies bind to the extracellular domain of GlyRs, ii) do not occlude the orthosteric binding sites of glycine or strychnine, and iii) favor either the active "open" channel conformation (19C8) or the resting "closed" channel (14E3) conformation, and that this conformational preference may be responsible for the resulting activating or inhibitory functional profiles, respectively. It is important to highlight that in our in vitro studies, the GlyRs were certainly desensitized as time-elapsed, similarly to that reported for AM-3607 (Huang et al., 2017), and that further structural studies would be required to fully define these functional profiles. A clear limitation in our current study is the lack of electrophysiology for these tool-antibodies. In fact, the long exposure times required in the in vitro assays rendered this very difficult to assess in cultured HEK293T cells and would ultimately be best evaluated in an ex-vivo rat spinal cord slice preparation to fully leverage the local neuronal circuitry that these channels govern. This fell outside of the scope of this work and should be evaluated later.

To further expand on the therapeutic possibilities of these tools, we evaluated their capability in crossing the BBB after a single intravenous administration. The brain to serum exposure ratios (0.4%–0.7%; Fig. 7, A and B) for mAbs 9A11 and 19C8 were somewhat higher than the range observed with most IgG1- or IgG2-type monoclonal antibodies (0.1%–0.2%) but consistent with reported values for antibodies that engage CNS targets, such as aducanumab (1.3% in Tg2576 transgenic mice) (Sevigny et al., 2016). More importantly, the absolute brain concentrations of either antibody were sufficient to cover their respective EC_{50}s (~1–3-fold) in the brain (Fig. 7C), suggesting the ability to elicit a pharmacological or toxicological response, based on existing small molecule data (see Huang et al., 2017 for an efficacious nonselective GlyRs small molecule in a chronic pain assay). As preliminary pharmacokinetic/tissue distribution studies demonstrated equal to or greater spinal cord exposure of each antibody relative to the brain (Supplemental Fig. 2) and both mAbs are expected to have similar distribution patterns, it can be postulated that significant target coverage in the spinal cord was achieved for both antibodies in the current study considering the reported expression of GlyRα1/3 in the rodent CNS (Harvey et al., 2004). We selected mAbs 9A11 and 19C8 as ideal proof-of-concept tool molecules based on similarities in their functional attributes (activators), brain-target coverage, and their dissimilarity in selectivity profile (for pain field perspective on this topic, see most recent review by Zeilhofer et al., 2021). We set out to compare their overall safety profile and therapeutic dose range and found that the selective antibody (mAb 9A11) had a safer overall profile when compared with the nonselective antibody (mAb 19C8) (Fig. 8). Interestingly, a similar (but less pronounced) effect was also noted on rearing (but not basic movement) in mice dosed with an efficacious (nonselective) GlyR small molecule potentiator AM-1488 with similar

target coverage (Bregman et al., 2017; Huang et al., 2017), implying a possible role for GlyRα1 in the reduced locomotor activity. Noteworthy, dose-dependent increases in the severity of labored breathing were observed with mAb 19C8, supporting the role of GlyRs in regulating respiration (Schmid et al., 1991; Bonham, 1995; Liu and Wong-Riley, 2013; Ghali, 2019). These data, in combination with the results seen by Huang et al. (2017), suggest that selectivity, although not required for efficacy, may be beneficial to alleviate limiting side effects of a potential therapeutic antibody. However, the efficacy of a GlyRα3 selective molecule has yet to be demonstrated and falls outside of the goal of this publication. Given the requirement for the 100 mg/kg dose necessary to achieve minimal target-coverage (as assessed by Huang et al., 2017), the observed side effects would limit an ability to perform a true dose-dependent efficacy study over a meaningful range of CNS target coverage. Increasing the potency of these tool antibodies or identifying another antibody with a similar selectivity profile and greater sensitivity (in pM range) would be necessary before efficacy assessment.

Together, our data demonstrate that in vitro HTS platform can be leveraged to identify a wide range of antibodies directed against Cys-Loop family of ligand-gated ion channels. In vitro, glycine receptor function can be modulated in a dose-dependent manner using high-affinity biologic tools, and despite the high protein homology between the GlyRα3 and α1 subunits, selectivity is achievable within this receptor family. In vivo, we demonstrate that the evaluated biologics can cross the rat BBB sufficiently enough to cover the therapeutic target at the concentrations up to 3-fold higher than the corresponding in vitro channel EC_{50}, and we show, for the first time, a benefit of selectivity of GlyRα3 over GlyRα1 to a potential therapeutic molecule's safety profile.

Acknowledgments

The authors would like to thank Daniel Cawley (Monoclonal Antibody Core Facility at Oregon Health and Science University) for his contributions in the development of the monoclonal antibodies employed in these studies. The authors are grateful to Philip Tagari and Amgen team for review of the manuscript and publication clearance, to Stefan McDonough for scientific guidance, Bill McCarty for insightful discussions on antibody biodistribution and to Dave Matson and Sonya Lehto for additional interpretation of in vivo behavioral studies. The following authors' new contact information is: Jeffrey R. Simard – C4 Therapeutics, Inc. (Waltham, MA), Klaus Michelsen – Relay Therapeutics (Cambridge, MA), Yan Wang – 2seventy bio (Cambridge, MA), Chunhua Yang – Atalanta Therapeutics (Boston, MA), Beth Youngblood – Epiodyne (San Francisco, CA), Barbara Grubinska- Takeda Pharmaceutical – (Cambridge, MA), Kristin Taborn – Wave Life Sciences (Cambridge, MA), Daniel J. Gillie – Fulcrum Therapeutics (Cambridge, MA), Brian E. Hall – Sanofi (Waltham, MA), Paul L. Shaffer – Janssen Pharmaceuticals, Inc. (Horsham, PA), Robert S. Foti – Merck (Boston, MA), Jacinthe Gingras – Homology Medicines, Inc. (Bedford, MA).

Authorship Contributions

Participated in research design: Simard, Foti, Gingras.

Conducted experiments: Simard, Michelsen, Wang, Yang, Grubinska, Taborn, Gillie, Cook, Chung, Hall.

Contributed new reagents or analytic tools: Long, Shaffer.

Performed data analysis: Simard, Michelsen, Wang, Yang, Grubinska, Taborn, Gillie, Cook, Chung.

Wrote or contributed to the writing of the manuscript: Simard, Foti, Gingras.

References

Ahmadi S, Lippross S, Neuhuber WL, and Zeilhofer HU (2002) PGE(2) selectively blocks inhibitory glycinergic neurotransmission onto rat superficial dorsal horn neurons. *Nat Neurosci* **5**:34–40.

Bagal SK and Bungay PJ (2012) Minimizing drug exposure in the CNS while maintaining good oral absorption. *ACS Med Chem Lett* **3**:948–950.

Beck A, Wurch T, Bailly C, and Corvaia N (2010) Strategies and challenges for the next generation of therapeutic antibodies. *Nat Rev Immunol* **10**:345–352.

Betz H and Laube B (2006) Glycine receptors: recent insights into their structural organization and functional diversity. *J Neurochem* **97**:1600–1610.

Beyer C, Roberts LA, and Komisaruk BR (1985) Hyperalgesia induced by altered glycinergic activity at the spinal cord. *Life Sci* **37**:875–882.

Bonham AC (1995) Neurotransmitters in the CNS control of breathing. *Respir Physiol* **101**:219–230.

Bosmans F and Swartz KJ (2010) Targeting voltage sensors in sodium channels with spider toxins. *Trends Pharmacol Sci* **31**:175–182.

Bregman H, Simard JR, Andrews KL, Ayube S, Chen H, Gunaydin H, Guzman-Perez A, Hu J, Huang L, Huang X, et al. (2017) The discovery and hit-to-lead optimization of tricyclic sulfonamides as potent and efficacious potentiators of glycine receptors. *J Med Chem* **60**:1105–1125.

Burgos CF, Yévenes GE, and Aguayo LG (2016) Structure and pharmacologic modulation of inhibitory glycine receptors. *Mol Pharmacol* **90**:318–325.

Chang HY, Wu S, Meno-Tetang G, and Shah DK (2019) A translational platform PBPK model for antibody disposition in the brain. *J Pharmacokinet Pharmacodyn* **46**:319–338.

Crisp SJ, Dixon CL, Jacobson L, Chabrol E, Irani SR, Leite MI, Leschziner G, Slaght SJ, Vincent A, and Kullmann DM (2019) Glycine receptor autoantibodies disrupt inhibitory neurotransmission. *Brain* **142**:3398–3410.

Dodd RB, Wilkinson T, and Schofield DJ (2018) Therapeutic monoclonal antibodies to complex membrane protein targets: antigen generation and antibody discovery strategies. *BioDrugs* **32**:339–355.

Foster E, Wildner H, Tudeau L, Haueter S, Ralvenius WT, Jegen M, Johannssen H, Hösli L, Haenraets K, Ghanem A, et al. (2015) Targeted ablation, silencing, and activation establish glycinergic dorsal horn neurons as key components of a spinal gate for pain and itch. *Neuron* **85**:1289–1304.

Ghali MGZ (2019) Respiratory rhythm generation and pattern formation: oscillators and network mechanisms. *J Integr Neurosci* **18**:481–517.

Gosselet F, Loiola RA, Roig A, Rosell A, and Culot M (2021) Central nervous system delivery of molecules across the blood-brain barrier. *Neurochem Int* **144**:104952.

Harvey RJ, Depner UB, Wässle H, Ahmadi S, Heindl C, Reinold H, Smart TG, Harvey K, Schütz B, Abo-Salem OM, et al. (2004) GlyR alpha3: an essential target for spinal PGE2-mediated inflammatory pain sensitization. *Science* **304**:884–887.

Hejazi N, Zhou C, Oz M, Sun H, Ye JH, and Zhang L (2006) Delta9-tetrahydrocannabinol and endogenous cannabinoid anandamide directly potentiate the function of glycine receptors. *Mol Pharmacol* **69**:991–997.

Hibbs RE and Gouaux E (2011) Principles of activation and permeation in an anion-selective Cys-loop receptor. *Nature* **474**:54–60.

Huang X, Chen H, Michelsen K, Schneider S, and Shaffer PL (2015) Crystal structure of human glycine receptor-α3 bound to antagonist strychnine. *Nature* **526**:277–280.

Huang X, Shaffer PL, Ayube S, Bregman H, Chen H, Lehto SG, Luther JA, Matson DJ, McDonough SI, Michelsen K, et al. (2017) Crystal structures of human glycine receptor α3 bound to a novel class of analgesic potentiators. *Nat Struct Mol Biol* **24**:108–113.

Hutchings CJ, Colussi P, and Clark TG (2019) Ion channels as therapeutic antibody targets. *MAbs* **11**:265–296.

Jensen AA and Kristiansen U (2004) Functional characterisation of the human alpha1 glycine receptor in a fluorescence-based membrane potential assay. *Biochem Pharmacol* **67**:1789–1799.

Liu Q and Wong-Riley MT (2013) Postnatal development of glycine receptor subunits α1, α2, α3, and β immunoreactivity in multiple brain stem respiratory-related nuclear groups of the rat. *Brain Res* **1538**:1–16.

Loomis CW, Khandwala H, Osmond G, and Hefferan MP (2001) Coadministration of intrathecal strychnine and bicuculline effects synergistic allodynia in the rat: an isobolographic analysis. *J Pharmacol Exp Ther* **296**:756–761.

Lynch JW and Callister RJ (2006) Glycine receptors: a new therapeutic target in pain pathways. *Curr Opin Investig Drugs* **7**:48–53.

Maleeva G, Buldakova S, and Bregestovski P (2015a) Ginkgolic acid specifically potentiates alpha 1 glycine receptors. *Springerplus* **4** (Suppl 1):L31.

Maleeva G, Buldakova S, and Bregestovski P (2015b) Selective potentiation of alpha 1 glycine receptors by ginkgolic acid. *Front Mol Neurosci* **8**:64.

Overington JP, Al-Lazikani B, and Hopkins AL (2006) How many drug targets are there? *Nat Rev Drug Discov* **5**:993–996.

Sarva H, Deik A, Ullah A, and Severt WL (2016) Clinical spectrum of stiff person syndrome: a review of recent reports. *Tremor Other Hyperkinet Mov (N Y)* **6**:340.

Schmid K, Böhmer G, and Gebauer K (1991) Glycine receptor-mediated fast synaptic inhibition in the brainstem respiratory system. *Respir Physiol* **84**:351–361.

Sevigny J, Chiao P, Bussière T, Weinreb PH, Williams L, Maier M, Dunstan R, Salloway S, Chen T, Ling Y, et al. (2016) The antibody aducanumab reduces Aβ plaques in Alzheimer's disease. *Nature* **537**:50–56.

Shalaly ND, Aneiros E, Blank M, Mueller J, Nyman E, Blind M, Dabrowski MA, Andersson CV, and Sandberg K (2015) Positive modulation of the glycine receptor by means of glycine receptor-binding aptamers. *J Biomol Screen* **20**:1112–1123.

Sun H and Li M (2013) Antibody therapeutics targeting ion channels: are we there yet? *Acta Pharmacol Sin* **34**:199–204.

Thomas P and Smart TG (2005) HEK293 cell line: a vehicle for the expression of recombinant proteins. *J Pharmacol Toxicol Methods* **51**:187–200.

Tyagarajan SK and Fritschy JM (2014) Gephyrin: a master regulator of neuronal function? *Nat Rev Neurosci* **15**:141–156.

Werynska K, Gingras J, Benke D, Scheurer L, Neumann E, and Zeilhofer HU (2021) A Glra3 phosphodeficient mouse mutant establishes the critical role of protein

kinase A-dependent phosphorylation and inhibition of glycine receptors in spinal inflammatory hyperalgesia. *Pain* **162**:2436–2445.
Wilkinson TC, Gardener MJ, and Williams WA (2015) Discovery of functional antibodies targeting ion channels. *J Biomol Screen* **20**:454–467.
Xiong W, Cheng K, Cui T, Godlewski G, Rice KC, Xu Y, and Zhang L (2011) Cannabinoid potentiation of glycine receptors contributes to cannabis-induced analgesia. *Nat Chem Biol* **7**:296–303.
Yaksh TL (1989) Behavioral and autonomic correlates of the tactile evoked allodynia produced by spinal glycine inhibition: effects of modulatory receptor systems and excitatory amino acid antagonists. *Pain* **37**:111–123.
Yévenes GE and Zeilhofer HU (2011) Molecular sites for the positive allosteric modulation of glycine receptors by endocannabinoids. *PLoS One* **6**:e23886.
Zeilhofer HU, Acuña MA, Gingras J, and Yévenes GE (2018) Glycine receptors and glycine transporters: targets for novel analgesics? *Cell Mol Life Sci* **75**:447–465.
Zeilhofer HU, Werynska K, Gingras J, and Yévenes GE (2021) Glycine receptors in spinal nociceptive control-an update. *Biomolecules* **11**:846.

Address correspondence to: Dr. Jacinthe Gingras, Homology Medicines, 1 Patriots Park, Bedford, MA 01730. Email: jgingras@homologymedicines.com; or Dr. Jeffrey R. Simard, C4 Therapeutics, 490 Arsenal Way, Suite 200, Watertown, MA 02472. Email: jsimard@c4therapeutics.com